Stochastic Technology Diffusion on Networks: A Network SAR Model

Ye-eun Song

Januray 2026

Abstract

We study a stochastic model of technology diffusion on networks using a Susceptible–Active–Removed (SAR) model. Using Gillespie simulation on Erdős–Rényi (ER) and Barabási–Albert (BA) networks with average degree $\langle k \rangle \approx 10$, we sweep the adoption rate β while keeping the churn rate γ and re-adoption rate ρ fixed. We quantify both typical behavior and variability using trajectory quantiles, peak-adoption distributions, the variance of peak adoption as a function of β, and success probability under multiple thresholds θ. We find a sharp transition between failure and takeoff, with strongest fluctuations in the critical region, and dependence on network topology.

1 Introduction

The adoption and decline of technologies often exhibit very different outcomes: some technologies exhibit rapid takeoffs while others fail. In this project, we investigate a minimal stochastic diffusion model on networks and ask:

> *How do network topology and technology adoption rate control technology diffusion trajectories and the variability of outcomes?*

We compare ER (homogeneous degree) and BA (heterogeneous degree with hubs) networks, focusing on ensemble-level statistics and identifying a critical region where small changes in parameters can lead to large changes in outcomes.

2 Model and Methods

2.1 Network SAR dynamics

Each node is in one of three states:

$$S \text{ (susceptible)}, \qquad A \text{ (active adopter)}, \qquad R \text{ (removed / inactive)}.$$

Transitions occur stochastically with rates:

$$S \to A: \quad \text{rate } \beta \cdot E_{SA}(t), \tag{1}$$

$$A \to R: \quad \text{rate } \gamma \cdot A(t), \tag{2}$$

$$R \to A: \quad \text{rate } \rho \cdot R(t), \tag{3}$$

where $E_{SA}(t)$ is the number of S–A edges at time t and $A(t), R(t)$ are the counts of nodes in those states.

The total event rate is

$$W(t) = \beta\, E_{SA}(t) + \gamma\, A(t) + \rho\, R(t). \tag{4}$$

The mean residence times implied by exponential waiting times are

$$\mathbb{E}[T_A] = \frac{1}{\gamma}, \qquad \mathbb{E}[T_R] = \frac{1}{\rho}. \tag{5}$$

(For $\gamma = 0.02$ and $\rho = 0.005$, these correspond to $\mathbb{E}[T_A] = 50$ months and $\mathbb{E}[T_R] = 200$ months.)

2.2 Simulation algorithm

We use the Gillespie (residence-time) algorithm on a fixed network:

- At each step, compute $W(t)$ and sample the time increment $\Delta t \sim \text{Exp}(W(t))$.
- Choose which event occurs with probabilities proportional to the three rates in Eqs. (1)–(3).
- Update states, update edge counts, and record $A(t)/N$ on a monthly grid.

2.3 Experimental design

We use:

- Network size: $N = 10{,}000$, mean degree $\langle k \rangle \approx 10$.
- Two topologies: ER (Erdős–Rényi) and BA (Barabási–Albert).
- Initial condition: $A(0) = A_0 = 10$, $R(0) = 0$, $S(0) = N - A_0$.
- Horizon: $T = 200$ months.
- Ensemble size: $K = 200$ independent runs per (network, β).
- Parameters: $\gamma = 0.02$, $\rho = 0.005$; adoption rate β is swept.

2.4 Summary statistics

Trajectory quantiles. For each month t, we compute the median and interquartile range (IQR) across runs:

$$A_{\text{med}}(t) = \text{median}_i \left(\frac{A_i(t)}{N} \right), \quad A_q(t) = \text{quantile}_i \left(\frac{A_i(t)}{N}; q \right), \; q \in \{0.25, 0.75\}.$$

Peak adoption. For run i we define peak adoption

$$A_{\max}^{(i)} = \max_{t \in [0,T]} \frac{A_i(t)}{N}. \tag{6}$$

and study its distribution and the variance across runs:

$$\text{Var}(A_{\max}) = \frac{1}{K-1} \sum_{i=1}^{K} \left(A_{\max}^{(i)} - \overline{A_{\max}} \right)^2. \tag{7}$$

Success probability and threshold robustness. Given a threshold θ, define success as $\{A_{\max}^{(i)} \geq \theta\}$. Then

$$P_{\text{success}}(\beta; \theta) = \frac{1}{K} \sum_{i=1}^{K} \mathbf{1}\left[A_{\max}^{(i)} \geq \theta \right]. \tag{8}$$

Binomial standard error for P_{success}. Treating the K runs as Bernoulli trials with empirical probability $\hat{p} = P_{\text{success}}$, the binomial standard error is

$$\text{SE}(\hat{p}) = \sqrt{\frac{\hat{p}(1-\hat{p})}{K}}. \tag{9}$$

We show ± 1SE error bars in plots.

3 Results

3.1 Ensemble trajectories: median and IQR

Figure 1 shows $A(t)/N$ median and IQR for ER vs BA at representative β values. At low β, adoption remains near zero and trajectories show strong variability at small scales. As β increases, trajectories exhibit rapid growth and subsequent decay toward a long-lived active fraction (influenced by churn γ and re-adoption ρ). Network topology shapes both the timing and magnitude of adoption as well as the variability of outcomes.

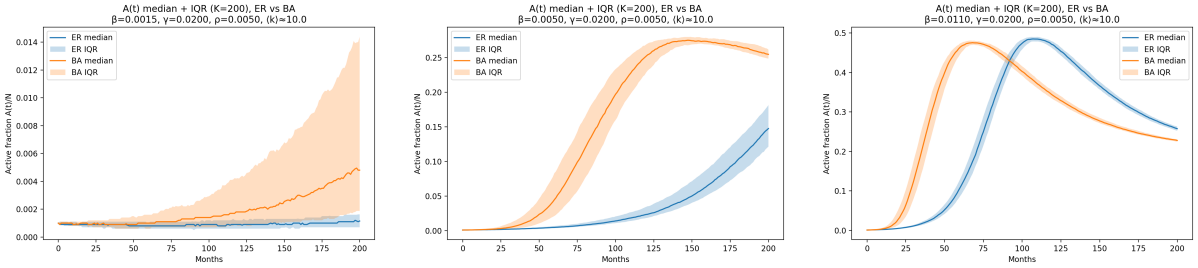

(a) Low adoption rate ($\beta = 0.0015$)

(b) Intermediate adoption rate ($\beta = 0.005$)

(c) High adoption rate ($\beta = 0.011$)

Figure 1: Median and interquartile range (IQR) of the active fraction $A(t)/N$ over $K = 200$ stochastic realizations for Erdős–Rényi (ER) and Barabási–Albert (BA) networks.

3.2 Peak adoption distributions

To measure how variable the outcomes are, we analyze the distribution of peak adoption. For each trajectory, the peak adoption is defined as the largest active fraction reached during the simulation, $A_{\max} = \max_t A(t)/N$. Figure 2 shows peak adoption histograms for Erdős–Rényi (ER) and Barabási–Albert (BA) networks at $\beta = 0.0025$.

For BA networks, the distribution is wide and strongly skewed to the right. This suggests strong run-to-run variability. A likely explanation is hub-driven amplification: when highly connected nodes become active early, they can initiate large cascades, whereas runs that do not activate hubs stay limited.

In contrast, ER networks display a much narrower distribution, with peak adoption values clustered at low levels. Since ER networks lack hubs, early random fluctuations are less likely to grow with $\beta = 0.0025$.

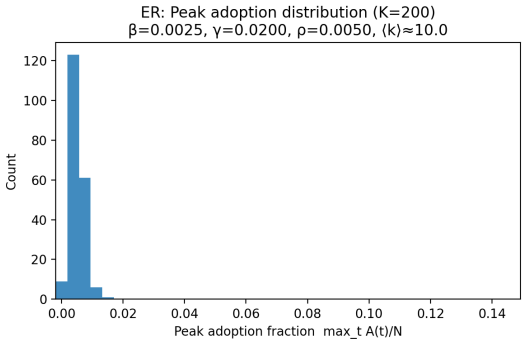

(a) ER

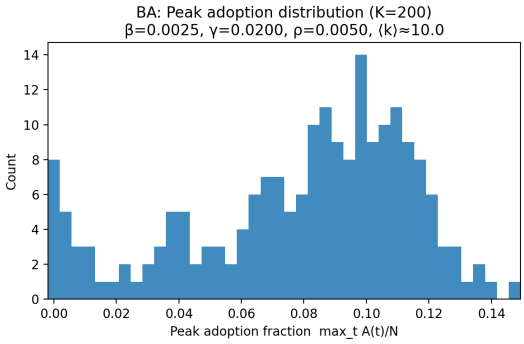

(b) BA

Figure 2: Peak adoption distributions at $\beta = 0.0025$ for ER and BA networks ($K = 200$ realizations).

3.3 Critical region via variance of peak adoption

To quantify the magnitude of run-to-run fluctuations, we consider the variance of the peak adoption fraction,

$$A_{\max}^{(i)} = \max_{t\in[0,T]} \frac{A^{(i)}(t)}{N},$$

across K stochastic realizations. The variance is defined as

$$\mathrm{Var}(A_{\max}) = \frac{1}{K-1}\sum_{i=1}^{K}\left(A_{\max}^{(i)} - \overline{A_{\max}}\right)^2, \tag{10}$$

where $\overline{A_{\max}}$ denotes the sample average of $A_{\max}$.

Figure 3 shows $\mathrm{Var}(A_{\max})$ as a function of the adoption rate β for Erdős–Rényi (ER) and Barabási–Albert (BA) networks. At small β, the variance is close to zero, reflecting consistent failure of adoption. Similarly, at large β, the variance is again small, corresponding to robust takeoff across nearly all realizations.

In contrast, an intermediate range of β exhibits a peak in $\mathrm{Var}(A_{\max})$, indicating stochastic fluctuations dominate the system behavior.

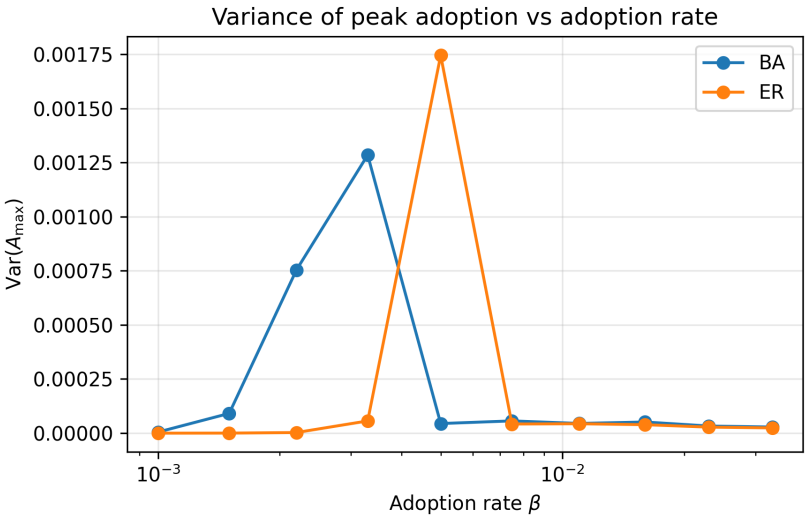

Figure 3: Variance of the peak adoption fraction, $\mathrm{Var}(A_{\max})$, as a function of the adoption rate β for Erdős–Rényi (ER) and Barabási–Albert (BA) networks.

3.4 Success probability and robustness to threshold

Figure 4 shows $P_{\text{success}}(\beta;\theta)$ for thresholds $\theta \in \{0.05, 0.15, 0.25\}$ with binomial standard error bars. For small β, success probability is near zero for all θ; for large β, it approaches one. For both ER and BA networks, P_{success} exhibits a sharp transition from near zero to near one as β increases.

BA networks systematically achieve high success probability at lower β than ER networks, reflecting the role of hubs in amplifying early stochastic activation. Binomial error bars peak near the transition region, consistent with maximal run-to-run variability at criticality.

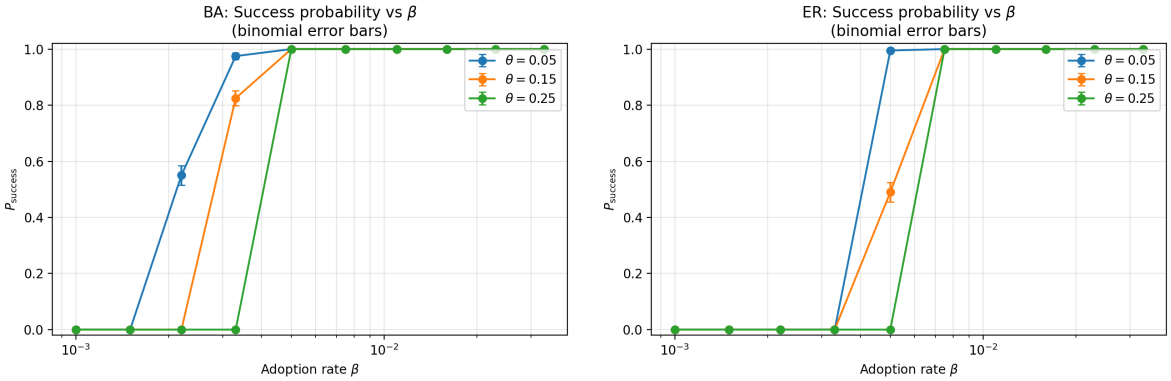

(a) BA (b) ER

Figure 4: Success probability vs β for multiple thresholds θ, with binomial standard error bars ($K = 200$).

3.5 Representative trajectories near the transition

To illustrate microscopic variability, we also plot a small subset of individual trajectories ($K = 10$) for selected β values (Fig. 5). These examples provide qualitative intuition about stochasticity of networked SAR models.

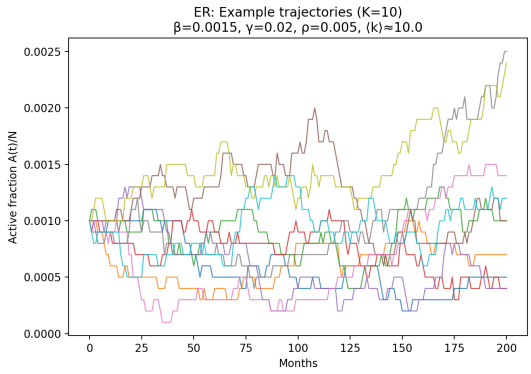

(a) ER, $\beta = 0.0015$

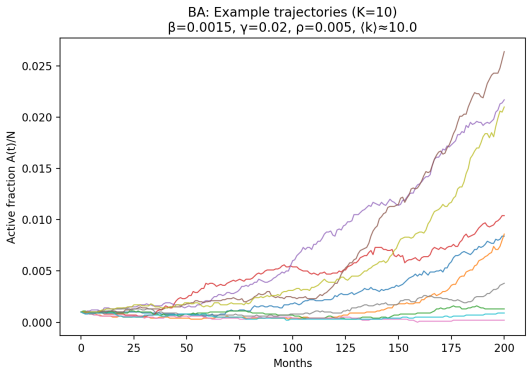

(b) BA, $\beta = 0.0015$

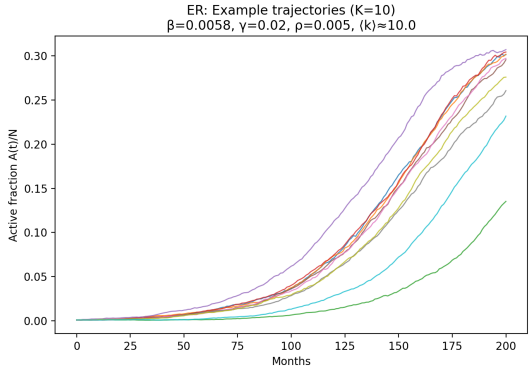

(c) ER, $\beta = 0.0058$

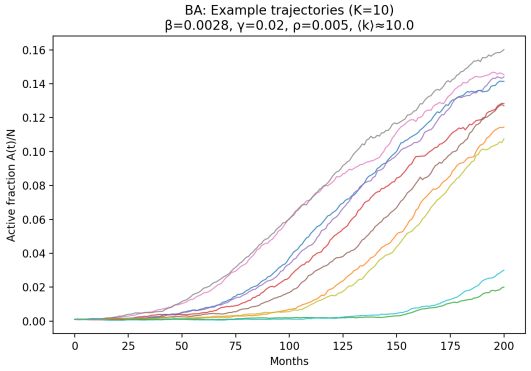

(d) BA, $\beta = 0.0028$

Figure 5: Peak adoption distributions for Erdős–Rényi (ER) and Barabási–Albert (BA) networks at multiple adoption rates.

4 Discussion

4.1 Interpretation

Our simulations reveal a clear transition from persistent failure to robust takeoff as the adoption rate β increases. This transition is not abrupt but occurs through a critical region characterized by large run-to-run fluctuations.

Network structure strongly shapes both typical outcomes and variability. Barabási–Albert (BA) networks, which contain hubs, exhibit earlier takeoff and larger fluctuations when stochasticity dominate in lower adoption rates compared to Erdős–Rényi (ER) networks.

In particular, hubs can act as amplification points: early stochastic activation of high-degree nodes can trigger large adoption cascades in some realizations, while their absence leads to failure in others. As a result, deterministic parameters alone do not uniquely determine outcomes near criticality; early-time stochastic events play a decisive role.

4.2 Relation to empirical Stack Overflow trends

We additionally consider Stack Overflow tag activity as a proxy for technology popularity over time (Fig. 6). Although these empirical data do not represent directly to the model variables or model structures, they provide an illustrative reference.

Normalized tag activity exhibits rapid growth, saturation, and gradual decline for different technologies, patterns that resemble simulation results in the model.

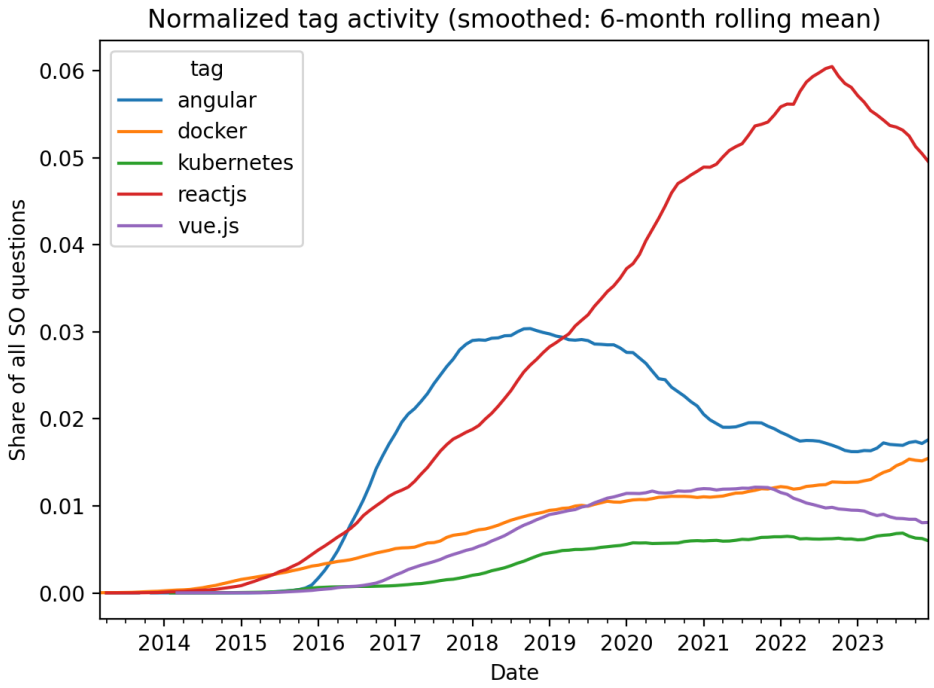

Figure 6: Normalized Stack Overflow tag activity (6-month rolling mean) for selected technologies. The time series illustrates qualitative patterns of technology adoption, takeoff, peak popularity, and decline.

4.3 Limitations and future work

This study intentionally adopts a minimal modeling framework, which entails several limitations.

First, networks are static and adoption parameters are homogeneous across nodes, whereas real social and technical networks evolve over time and exhibit strong heterogeneity. Second, the model does not include explicit competition or external shock effects. Lastly, the role of hubs for stochastic diffusion was not explicitly simulated for the BA models.

Future work could address these limitations by incorporating explicit modeling of hub-targeted dynamics or extending the framework to multiple competing technologies.

5 Conclusion

We studied stochastic technology diffusion on networks using a minimal Susceptible–Active–Removed (SAR) model simulated on Erdős–Rényi and Barabási–Albert graph topologies. By sweeping the adoption rate β and analyzing ensemble trajectories, peak adoption statistics, success probabilities, and fluctuations, we characterized the transition from failure to takeoff in networked diffusion processes.

Our results show that this transition occurs through a critical region marked by maximal variability in peak adoption. In this regime, identical parameter settings can lead to qualitatively different outcomes.

These findings demonstrate that simple stochastic models on networks can reproduce key qualitative features of technology adoption, including takeoff, failure, and sensitivity to early random events.

Bibliography

References

[1] R. Toral and P. Colet, *Stochastic Numerical Methods: An Introduction for Students and Scientists*, Wiley-VCH, Weinheim, Germany (2014).